Институт за физика

Physica Macedonica **61**, (2012) p. 113-119
ISSN 1409-7168

THE EFFECT OF ALUMINUM ON THE MICROSTRUCTURE AND MECHANICAL PROPERTIES OF ARC-EVAPORATED $Ti_{1-X}Al_XN$ COATINGS DEPOSITED ON CEMENTED CARBIDE SUBSTRATES

F. Aliaj[1], N. Syla[1], T. Dilo[2] and S. Avdiaj[1]

[1]*University of Prishtina, Faculty of Mathematical and Natural Sciences, Mother Theresa Street 5, 10000 Prishtina, Republic of Kosovo*

[2]*University of Tirana, Faculty of Natural Sciences, Bulevardi Zogu i Parë, Tirana, Albania*

Abstract. The effect of aluminum contents (x) on the microstructure and mechanical properties of cathodic arc evaporated $Ti_{1-x}Al_xN$ coatings was investigated. The coatings were deposited on mirror-polished plates of cemented carbides from mixed powder metallurgical $Ti_{1-xT}Al_{xT}$ targets with xT = 0.50, 0.55, 0.60 and 0.66. The depositions were performed in a N_2 atmosphere maintained at a working pressure of 5 Pa and at a bias voltage of -100 V. Glow discharge optical emission spectroscopy (GDOES), X-ray diffraction in glancing angle mode (GAXRD) and nano-indentation were used to characterize the chemical composition, the microstructure and the mechanical properties of the coatings. The results deduced from GDOES data analysis show that the coatings have a slightly higher aluminum contents than the targets used to deposit the coatings. The aluminum content was found to influence the phase composition, microstructure and mechanical properties of the coatings. The phase composition of the coatings changed from predominantly single-phase fcc-$Ti_{1-x}Al_xN$ for x between ~0.5 and ~0.6 to dual-phase fcc-$Ti_{1-x}Al_xN$ and w-AlN for x~0.66. For coatings with $x < 0.6$ the stress-free lattice parameter decreases with increasing x, whereas the hardness maintains a constant value of ~23 GPa. Further increasing the aluminum content is followed with an abrupt decrease in hardness by ~7 GPa.

PACS: 81.15.-z, 62.20.Qp, 61.10.Nz, 68.55.Nq

1. INTRODUCTION

The (Ti,Al)N coatings grown on the WC-Co substrates are multifunctional materials having a wide range of applications in various fields[1-3], owing to their excellent high hardness, wear resistance, high temperature oxidation/corrosion resistance, low coefficient of friction and low thermal conductivity. The cathodic arc evaporation (CAE) is an efficient and high productivity technique used for the deposition of (Ti,Al)N coatings [1,4-6], as it produces dense and adherent coatings and at high deposition rates. In this contribution, $Ti_{1-x}Al_xN$ coatings

were grown with CAE technique using powder metallurgical Ti-Al targets with different Al contents, and investigated with XRD, GDOES and nanoindentation experiments.

2. EXPERIMENTAL DETAILS

$Ti_{1-x}Al_xN$ coatings with different chemical compositions (x) were deposited on mirror-polished cemented carbide substrates (WC-Co) by cathodic arc evaporation (CAE) using a coating unit π300 from PLATIT. Different chemical compositions of the coatings were achieved by using PLANSEE targets $Ti_{1-xT}Al_{xT}$, produced by powder metallurgy, with different Al content: xT = 0.50, 0.55, 0.60 and 0.66. The deposition consisted of a heating and cleaning of the substrates, after which a thin aid-adherent base layer of TiN was deposited for 5 min in a nitrogen atmosphere with a pressure of 0.5 – 1.0 Pa. Then, the deposition of the main coating, which was done for 160 minutes in a nitrogen atmosphere with a working pressure of 5 Pa, followed. The deposition temperature was approx. 500 ^oC; the current on the target was 300 A, and a negative bias voltage of -100 V was applied to the substrate.

The chemical composition of the coatings was estimated by means of a glow discharge optical emission spectroscopy (GDOES) using a commercial surface depth profile instrument GDS-750A from Leco. The microstructure of the coatings was characterized by X-ray diffractometry in glancing angle configuration (GAXRD). The GAXRD experiments were done on a D8 Advance diffractometer, that was equipped with an X-ray tube with copper anode, with a Goebel mirror in the primary beam and with a Soller collimator and a flat LiF monochromator that were situated in the diffracted beam in front of the scintillation detector. The diffraction patterns were taken at an angle of incidence $\gamma = 3^o$ by scanning between 2θ values of $25 – 159^o$. The GAXRD experiments revealed information on the phase composition [6,7], crystallite size [8], stress-free lattice parameter [6,9], and residual stress [6,10].

The indentation hardness and Young's modulus of the coatings were measured by instrumented nanoindentation. Nanoindentation experiments were done in a CSM nano-hardness tester equipped with a Berkovich diamond indenter and considering the Oliver and Pharr method [11]. The experimental conditions are similar to those used in our previous work [7]. The coatings thickness was determined by Calotest method using a Compact Calotest instrument from CSM.

3. RESULTS AND DISCUSSION

In this study, $Ti_{1-x}Al_xN$ coatings with different Al content, x, deposited with CAE method showed a variety of characteristics, although they were prepared using the same deposition parameters.

Results of chemical composition deduced from GDOES analysis show that the Al content in the coatings is higher than that in the evaporation targets. From Table 1 we see that there is no relationship between the target composition and coatings thickness, for the chosen deposition parameters. Thus, we can conclude that the target composition has no effect on the

growth rate of the coatings. In our previous study [7] on the effect of bias voltage on the microstructure and mechanical properties of (Ti,Al)N coatings deposited with CAE, we have found that increasing bias voltage, and in this way the energy of the bombarding ions, while keeping other parameters constant had no effect in the growth rate and in the preferential incorporation of Al or Ti into the coatings. Similar results were obtained by Wüstefeld et al [12]. The mechanism behind Al enrichment in the coatings under study is attributed to the lower melting point of Al than Ti and to relatively large arc current used to deposit the coatings. The high arc current may give rise to arc spot splitting, which in turn may result in an increased evaporation rate of Al more so than Ti.

Part of the GAXRD patterns of the coatings investigated in this work is shown in Fig. 1. All the fcc-(Ti,Al)N peaks are shifted to higher diffraction angles than the standard value of fcc-TiN. This is due to the incorporation of the smaller Al atoms into the fcc-TiN lattice. The phase composition of the coatings was concluded from the presence of the diffraction peaks of the respective phases. In the TiAlN-1, TiAlN-2 and TiAlN-3 coatings the dominating phase is fcc-(Ti,Al)N, although there were peaks from fcc-AlN phase detected by GAXRD. The lattice parameter of the detected fcc-AlN peaks were in good agreement with PDF-2[13]. The TiAlN-4 coating exhibit a mixture of fcc-(Ti,Al)N phase and w-AlN phase with wurtzitic type structure. The Al content in this coating is ~0.68, which is slightly above the maximum solubility limit, which is ~0.65, of Al into fcc-(Ti,Al)N [20].

Table 1: Targets and coatings chemical composition, thickness and some microstructure parameters of the coatings investigated in this work

Sample number	**Target comp. (*x*T)**	**Coating comp. (*x*)**	**Coating thickness (*t*) (μm)**	**Stress-free lattice parameter (a_0) (nm)**	**Residual stress σ (GPa)**	**Crystall. size (*D*) (nm)**	**Mutual dis. (*w*) (°)**
TiAlN-1	0.50	0.522(5)	2.7(1)	0.41766(32)	-7.51(37)	4.7(2)	0.69(8)
TiAlN-2	0.55	0.570(12)	2.4(1)	0.41661(26)	-7.38(29)	4.4(1)	0.74(9)
TiAlN-3	0.60	0.618(3)	2.6(1)	0.41611(26)	-6.06(27)	3.4(1)	0.94(11)
TiAlN-4	0.66	0.676(3)	2.9(2)	0.41694(87)	-4.16(93)	---	---

The maximum solubility limit of Al in fcc-(Ti,Al)N depends on the PVD technique used to grow the film and is influenced primarily by the deposition parameters [14]. In a recent publication, Mayrhofer et al [15] have shown that the maximum solubility limit of Al in fcc-(Ti,Al)N can be varied from 0.64 – 0.74 by affecting the Al distribution in the metal sub-lattice. Therefore, the mechanism that influences the Al distribution during film growth can influence the phase stability of supersaturated fcc-(Ti,Al)N. The reduction of w-AlN phase and the presence of fcc-(Ti,Al)N phase in TiAlN-4 coating can be explained by the relatively high bias voltage applied at the substrate during deposition. The bias voltage controls the energy of ions arriving at the substrate. At high bias voltages the ion bombardment acts as the mechanism that influences the Al distribution during coating process, and thus helps the stabilization of fcc-(Ti,Al)N at Al contents larger than 0.65. Furthermore, the fcc-(Ti,Al)N can be stabilized at Al

content larger than the maximum solubility limit if the coatings are under a high compressive residual stress [12,16].

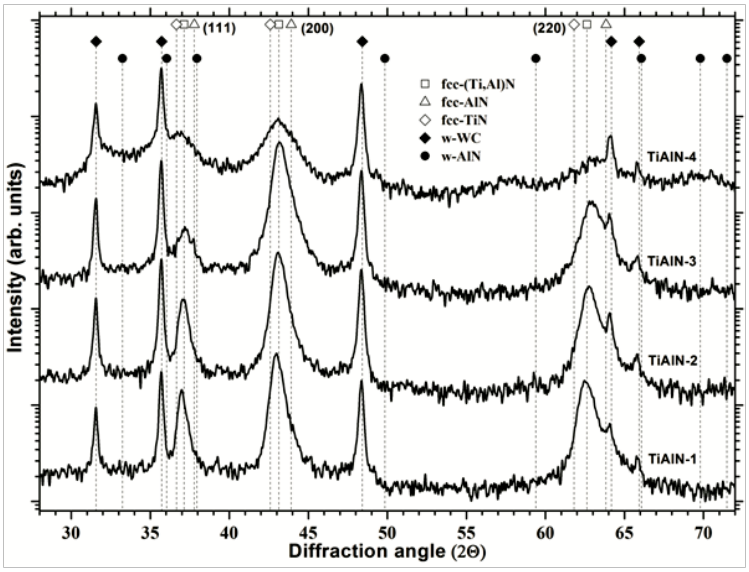

Fig. 1: GAXRD patterns of coatings investigated in this work. The vertical dotted lines indicate the peak positions for the expected phases. The positions of fcc-TiN, fcc-AlN, w-AlN and WC were taken from PDF-2 [13]. Positions of the fcc-(Ti,Al)N phase were calculated using Braggs' law and a value for lattice parameter a = 0.419 nm**.**

The relatively large compressive residual stress found in the TiAlN-4 coating may have additionally helped the stabilization of fcc-(Ti,Al)N phase. The effect of higher values of bias voltage on the phase composition was already observed for $Ti_{1-x}Al_xN$ [12] and Ti-Al-X-N (X = V and Ta) [16,17] coatings deposited by CAE technique.

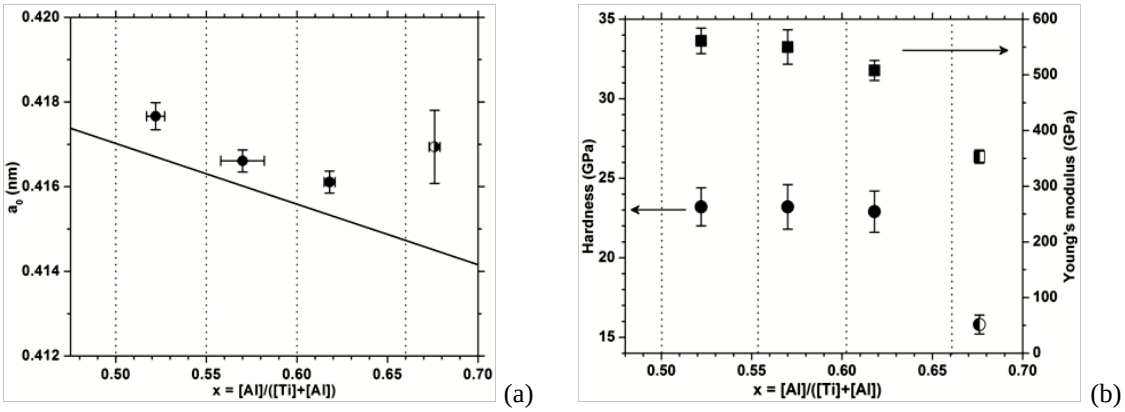

Fig. 2: (a) The dependence of the stress-free lattice parameter on the Al content. The solid line represents the anticipated Vegard-like dependence and the equation for this line is taken from [6]; (b) Hardness and Young's modulus of the coatings investigated in this work as a function of Al content. Vertical dotted lines represent the Al content of the targets used to deposit the coatings**.**

The stress-free lattice parameter, a_0, and the residual stress, σ, in the fcc-(Ti,Al)N phase were derived from the linear dependence of the lattice parameters of fcc-(Ti,Al)N on $\sin^2\psi$, as described in papers [6,9,10]. For the calculation of a_0 and σ, the Poisson ratio of ν = 0.3 and Young's modulus, as derived from nano-indentation measurements, were used. The dependence of the stress-free lattice parameter on Al content is shown in Fig. 2a. In the coatings were the dominating phase is fcc-(Ti,Al)N, the stress-free lattice parameter decreases with increasing Al content as expected. However, the measured stress-free lattice parameters are higher than the anticipated Vegard-like dependence of the intrinsic lattice parameter on the overall Al content in the coatings. This result indicates that the fcc-(Ti,Al)N phase contains less Al than corresponds to the overall chemical composition as measured from GDOES. As discussed by Rafaja et al [6], the aluminum, which is missing in the fcc-(Ti,Al)N, forms another phase. In TiAlN-1, TiAlN-2 and TiAlN-3 coatings this second phase is fcc-AlN, the presence of which was confirmed by GAXRD patterns. For the TiAlN-4 coating, that shows a mixture of fcc-(Ti,Al)N and w-AlN, the departure of stress-free lattice parameter from the anticipated Vegard-like dependence can be understood as a measure of the decomposition of fcc-$Ti_{1-x}Al_xN$ into fcc-$Ti_{1-x'}Al_{x'}N$, with $x' < x$, and w-AlN [19].

Residual stress in all the coatings was compressive (see Table 1). The largest values of compressive residual stress, approx. 6 – 8 GPa, are found for Al contents between ~0.5 and ~0.6, where the dominating phase is fcc-(Ti,Al)N. Increasing further the Al contents is followed with a rapid decrease of residual stress to about 4 GPa. This rapid decrease of residual stress when Al contents increases from ~0.60 to ~0.66 is related to the phase transition from fcc to a mixture of fcc+w. This phase transition is followed with a volume shrinkage in the AlN phase that generates tensile stresses, so the compressive residual stress in the fcc-(Ti,Al)N phase decreases sharply [18].

The dependence of indentation hardness and Young's modulus on the Al content is shown in Fig. 2b. The hardness and Young's modulus show the same trends with increasing Al contents. The largest values of hardness and Young's modulus, ~23 GPa and ~550 GPa respectively, are found in coatings where the dominating phase is fcc-(Ti,Al)N (x = ~0.5 – 0.6). The duals phase fcc-(Ti,Al)N/w-AlN present at higher Al contents exhibit much lower values of hardness and Young's modulus, ~16 GPa and ~350 GPa respectively. Therefore, it can be concluded that the rapid decrease in hardness and Young's modulus is related with the introduction of the hexagonal w-AlN phase. This correlation between residual stress, hardness and Young's modulus and the presence of w-AlN phase is frequently reported in literature [12,16,18].

All the GAXRD patterns of the coatings under study were fitted with Pearson-VII function by means of a peak-by-peak least-square refinement. This procedure was useful in determining several peak parameters, including the exact position, which made possible the evaluation of stress-free lattice parameters and residual stresses presented above, and line broadening. However, analysis of the dependence of XRD line broadening on the size of the diffraction vector showed that the coatings consist of partially coherent crystallites with very small mutual disorientation. This phenomenon of crystallographic coherence was described by

Rafaja et al [8] and was illustrated in many examples [6,9,10,19]. From the dependence of XRD line broadening on the size of the diffraction vector, with the aid of the procedure described in [8], three microstructure parameters were calculated: the average size of clusters which consisted of partially coherent fcc-(Ti,Al)N crystallites, the average size of crystallites and their mutual disorientation (see Table 1). It was found that the cluster size did not change, within experimental accuracy of the XRD line profile analysis, with the increase of Al content. The cluster size was only estimated to be between ~30 and ~100 nm. Furthermore, for the TiAlN-4 coating, the size of crystallites in fcc-(Ti,Al)N could not be determined, because peaks at higher 2θ angles were missing in this phase.

4. CONCLUSIONS

Based on the results presented above, the following can be concluded for the $Ti_{1-x}Al_xN$ coatings deposited on WC-Co substrates with CAE technique.

- The Al content in all the coatings was higher than in the cathode used to deposit the coatings;
- Al content was found to strongly influence the phase composition of the coatings. For x between ~0.5 and ~0.6 the dominating phase was fcc-(Ti,Al)N with some fcc-AlN peaks detected by XRD. Further increasing Al content to ~0.66 lead to the decomposition of fcc-$Ti_{1-x}Al_xN$ into fcc- $Ti_{1-x'}Al_{x'}N$, with $x' < x$, and w-AlN;
- Residual stress in all the coatings was compressive. For x between ~0.5 and ~0.6, the residual stress was approx. 6 – 8 GPa, while further increase of Al content resulted in a substantial reduction of residual stress due to the introduction of the hexagonal AlN phase;
- The indentation hardness and Young's modulus showed similar trends as residual stress, with largest values for x between ~0.5 and ~0.6, and with substantial reduction in the values when x is increased to ~0.66;
- The coatings were deposited in clusters, composed of partially coherent crystallites with very small mutual disorientation $w < 1^o$. While Al content was found to have no effect on the cluster size, the size of crystallites decreased slowly with increasing Al content.

REFERENCES

[1] B. F. Coil, P. Sathrum, R. Fontana, J. P. Peyre, D. Duchateau and M. Benmalek, Surf. Coat. Technol. **52** (1992)

[2] G. Håkansson, J.-E. Sundren, D. McIntyre, J. E. Greene and W.-D. Münz, Thin Solid Films **153** (1987)

[3] H.G. Prengel, P.C. Jindal, K.H. Wendt, A.T. Santhanam, P.L. Hegde, R.M. Penich, Surf. Coat. Technol. **139** (2001)

[4] M. Ahlgren and H. Blomqvist, Surf. Coat. Technol. **200** (2005)

[5] A.C. Vlasveld, S.G. Harris, E.D. Doyle, D.B Lewis, W.D. Munz, Surf. Coat. Technol. **149** (2002)

[6] D. Rafaja, C.Wüstefeld, C. Bähtz, V. Klemm,M. Dopita,M. Motylenko, C. Michotte and M. Kathrein, Metal. Mater. Trans. A, **42(3)** (2011)

[7] F. Aliaj, N. Syla, S. Avdiaj, T. Dilo, "The effect of bias voltage on the microstructure and mechanical properties of arc evaporated (Ti,Al)N hard coatings" – In publication process, Bull. Mater. Sci., Vol. 35, No. 9, December 2012
[8] D. Rafaja, V. Klemm, G. Schreiber, M. Knapp, R. Kužel, J. Appl. Cryst. **37** (2004)
[9] D. Rafaja, C. Wüstefeld, M. Dopita, V. Klemm, D. Heger, G. Schreiber, M. Šíma, Surf. Coat. Technol. **203** (2008)
[10] D. Rafaja, M. Dopita, M. Růžička, V. Klemm, D. Heger, G. Schreiber, M. Šíma, Surf. Coat. Technol. **201** (2006)
[11] W.C. Oliver, G.M. Pharr, J. Mater. Res. **7** (1992)
[12] Ch. Wüstefeld, D. Rafaja, V. Klemm, C. Michotte, M. Kathrein, Surf. Coat. Technol. **205** (2010)
[13] PDF-2, PowderDiffraction File, ICDD, Philadelphia, PA, 1997.
[14] S. PalDey, S.C. Deevi, Mater. Sci. Eng. **A342** (2002)
[15] P. H. Mayrhofer, D. Music, and J. M. Schneider, J. Appl. Phys. **100** (2006)
[16] M. Pfeiler, K. Kutschej, M. Penoy, C. Michotte, C. Mitterer, M. Kathrein, Surf. Coat. Technol. **202** (2007)
[17] M. Pfeiler, G. A. Fontalvo, J. Wagner, K. Kutschej, M. Penoy, C. Michotte, C. Mitterer, M. Kathrein, Tribol. Lett. **30** (2008)
[18] Min Zhou, Y. Makino, M. Nose, K. Nogi, Thin Solid Films **339** (1999)
[19] D. Rafaja, A. Poklad, V. Klemm, G. Schreiber, D. Heger, M. Šíma, M. Dopita, Thin Solid Films **514** (2006)
[20] A. Sugishima, H. Kajioka, Y. Makino, Surf. Coat. Technol. **97** (1997)